minerals

MDPI

Article

Synchrotron Radiation XRD Investigation of the Fine Phase Transformation during Synthetic Chalcocite Acidic Ferric Sulfate Leaching

Chaojun Fang [1,2], Shichao Yu [1,2], Xingxing Wang [1,2], Hongbo Zhao [1,2], Wenqing Qin [1,2], Guanzhou Qiu [1,2] and Jun Wang [1,2,*]

1 School of Minerals Processing and Bioengineering, Central South University, Changsha 410083, China; fangchaojun1009@126.com (C.F.); yushichao@csu.edu.cn (S.Y.); wangxingxing@csu.edu.cn (X.W.); alexandercsu@126.com (H.Z.); qinwenqing@csu.edu.cn (W.Q.); qgz@csu.edu.cn (G.Q.)

2 Key Lab of Bio-hydrometallurgy of Ministry of Education, Changsha 410083, China

* Correspondence: wjwq2000@126.com; Tel.: +86-731-88876557

Received: 7 August 2018; Accepted: 12 October 2018; Published: 17 October 2018

Abstract: The fine phase transformation process of chalcocite (Cu_2S) leaching in acidic ferric sulfate solution was studied by leaching experiments and synchrotron radiation X-ray diffraction (SRXRD) tests. The results showed that the dissolution process of chalcocite was divided into two stages. In the first stage, Cu_2S was firstly transformed to Cu_5FeS_4 and $Cu_{2-x}S$, then the galvanic effect between Cu_5FeS_4 and $Cu_{2-x}S$ accelerated the dissolution process of $Cu_{1.8}S \rightarrow Cu_{1.6}S \rightarrow CuS$, and finally Cu_5FeS_4 was also transformed to CuS. While in the second stage, CuS was transformed to elemental sulfur, which formed the passivation layer and inhibited the leaching of chalcocite. Specifically, Cu_5FeS_4 was detected during the chalcocite leaching process by SRXRD for the first time. This research is helpful for revealing the detailed leaching process of chalcocite.

Keywords: synchrotron radiation; SRXRD; chalcocite; leaching; ferric ions

1. Introduction

Flotation is one of the most important methods for primary enrichment of minerals and it has significantly developed in recent years [1–4]. However, hydrometallurgy, particularly bioleaching, has the advantages of being simple, low cost, and eco-friendly, which has been successfully applied in the processing of low grade minerals all over the world [5–11]. However, there are still some problems and challenges in the leaching of secondary copper sulfide minerals. The phase transformation mechanism and dissolution kinetics of chalcocite are not clear, which is considered as the main reason for low leaching efficiency and an unsatisfactory leaching rate [12–15]. Therefore, it is necessary to reveal the detailed dissolution mechanism and promote the copper leaching rate.

The crystal structure of chalcocite is more complex than its simple composition. High chalcocite belongs to the $P_{6\text{-}3}/mmc$ space group, in which sulfur atoms are arranged in hexagonal close-packing order, whilst three varieties of copper atoms with four-fold, three-fold, and two-fold coordination are randomly packed in the interstices of sulfur atoms [16]. The structures of low chalcocite and djurleite are derived from the high chalcocite structure and both are monoclinic [17]. It was reported that the structure of low chalcocite was either disordered or belonged to the Pc space group, with four of the 96 copper atoms taking on two-fold coordination in the monoclinic unit. The structure of djurleite is in space group $P_{2\text{-}1}/n$ and with a unit cell containing 8 $Cu_{31}S_{16}$, it is in general similar to low chalcocite. However, there are 62 different copper atoms, where 52 are in three-fold and triangular coordination with sulfur, 9 form a distorted tetrahedral group, and 1 is in linear coordination [18]. In addition,

compared with structural data of other copper-rich sulfides, the tetrahedral, triangular, and linear Cu-S bond of low chalcocite and djurleite are of large distortions and wide variations in bond lengths [19].

Many publications show that the dissolved process of chalcocite acidic ferric sulfate leaching can be divided into two stages, with the production of secondary covellite as an intermediate (Equations (1) and (2)) [13,20–26], whilst ferric ions were regenerated by Equation (3).

$$Cu_2S + 2Fe^{3+} \rightarrow Cu^{2+} + 2Fe^{2+} + CuS \quad (1)$$

$$CuS + 2Fe^{3+} \rightarrow Cu^{2+} + 2Fe^{2+} + S^0 \quad (2)$$

$$4Fe^{2+} + O_2 + 4H^+ \rightarrow 4Fe^{3+} + 2H_2O \quad (3)$$

The leaching rate of the first stage of chalcocite ferric leaching is very fast compared with the second stage. However, there exists several phase transformation processes in the first stage of leaching. It is reported that chalcocite would be transformed to djurleite ($Cu_{1.97}S$), digenite ($Cu_{1.8}S$), anilite ($Cu_{1.75}S$), geerite ($Cu_{1.6}S$), spionkopite ($Cu_{1.4}S$), yarrowite ($Cu_{1.12}S$), and covellite (CuS) in that order [27–29]. According to the stoichiometry, when copper extraction reached 10%, chalcocite would disappear and transform to digenite, whilst all the intermediates were transformed to covellite when copper extraction achieved 50%.

In essence, the second stage is the oxidative dissolution of the secondary covellite, in which the elemental sulfur and Cu^{2+} are produced. It is reported that the secondary covellite has more chemical activity than the primary covellite, which may be attributed to the increasing surface area formed by the first stage of chalcocite leaching [24,30].

The dissolution behavior of the sulfur element in chalcocite ferric leaching is an important output of this mechanism. Chalcocite and covellite can be attacked by Fe^{3+}, O_2, and H^+ attributed to its acid-soluble properties. However, different from the four dissolution pathways (metal-deficient sulfides, polysulfide, element sulfur, and jarosites) of chalcopyrite [31–38], the dissolution of sulfur element in the second stage of chalcocite ferric leaching follows the polysulfide pathway and elemental sulfur is formed [24].

Synchrotron radiation (SR) has the advantages of high-brilliance and flux, wide energy spectrum, very short pulses, and high purity, and many scientific problems could be resolved by SR-based technologies. There are three synchrotron radiation facilities in China to date, Beijing Synchrotron Radiation Facility (BSRF), Shanghai Synchrotron Radiation Facility (SSRF), and the National Synchrotron Radiation Laboratory (NSRL). In the mineral processing and hydrometallurgy research field, SR-based technologies such as SRXRD, SRXPS, and XANES were mainly used to study the fine phase transformation and variation of chemical substances on the mineral surface [39–45]. In this paper, synthetic chalcocite was chosen as the research object, and SRXRD was employed to explore the fine phase transformation mechanism in chalcocite acidic ferric sulfate leaching. The results would be helpful for explaining the key chemical reactions and key intermediates in chalcocite leaching, and finally to improve copper extraction and resource utilization of secondary copper sulfide minerals.

2. Materials and Methods

2.1. Mineral

The chalcocite sample used in experiments was bought from Sinopharm Chemical Reagent Co., Shanghai, China. The purchased chalcocite was ground using a laboratory mill and sieved to the size of ~0.074 mm for leaching experiments and SRXRD tests.

Chalcocite was confirmed by chemical composition analysis and an SRXRD test. The SRXRD test was completed in beamline 4B9A at the Beijing Synchrotron Radiation Facility (BSRF, Beijing, China). Figure 1 shows that the SRXRD peaks of the sample were fitted with the peaks of chalcocite. Table 1 shows that the contents of copper element and sulfur element were 78.61% and 18.95%, respectively. The results indicated that chalcocite sample used in this paper was of high purity.

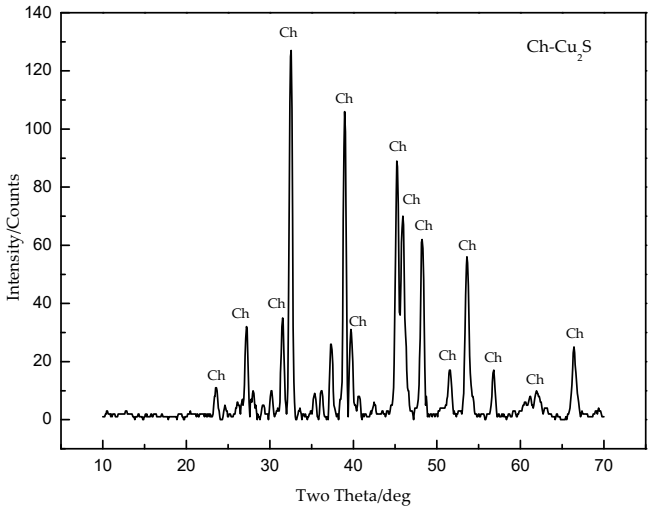

Figure 1. Synchrotron radiation X-ray diffraction (SRXRD) results of synthetic chalcocite samples (BSRF).

Table 1. Chemical compositions analysis results of chalcocite (%).

Sample	Cu	S	Fe	Ca	Si
Chalcocite	78.61	18.95	0.018	0.017	0.053

2.2. Leaching Experiments

One gram of chalcocite with a size of ~0.074 mm was put into a 250 mL shake flask containing 100 mL of sterilized distilled water, and then two grams of ferric sulfate hydrate ($Fe_2(SO_4)_3 \cdot xH_2O$) was added as the source of ferric ions. The pH value was adjusted to 1.7 by diluting sulfuric acid and then the shake flasks were placed into an orbital shaker at a speed of 170 rpm and temperature of 45 °C. The shake flask was sealed with a breathable sealing film to prevent rapid evaporation of water, and the atmosphere inside the orbital shaker was standard atmospheric air and the oxygen in the air could enter the shake flask.

In the leaching process, the pH value was adjusted back to 1.7 when it was above 2.0, and water lost by evaporation was supplemented periodically by distilled water regularly. Copper ion concentrations and iron ion concentrations were measured with an inductively coupled plasma-atomic emission spectrometer (ICP-AES) (PS-6, Baird Co., Deford, MA, USA). The redox potentials of the leaching solution were determined by a Pt electrode with reference to an Ag/AgCl electrode (3.0 mol/L KCl) (BPH-221, Dalian BELL Co., Dalian, China), whilst the pH values were measured with a pH meter (PHSJ-4A, Shanghai LEICI Co., Shanghai, China).

The leaching experiments were set as multiple parallel samples, and the samples were removed according to the time set in advance. The removed sample was filtered with a neutral filter paper and cleaned with distilled water three times, afterwards, the samples were dried in a vacuum oven for 24 h for the tests of SRXRD.

2.3. Synchrotron Radiation X-ray Diffraction

The SRXRD spectra were obtained from beamline BL14B1 of the Shanghai Synchrotron Radiation Facility (SSRF). The amount of mixed sample that needed to be added for each test was 50 mg. The wavelength of incident synchrotron radiation X-ray was 0.6895 nm, and the SRXRD spectra ranged from 4° to 38°. The background removal and phase comparison of the spectra were completed using the software Jade 6.

3. Results and Discussion

3.1. Leaching Behaviors

The copper extraction of chalcocite leaching at different leaching times is shown in Figure 2a. It indicated that the leaching of chalcocite was divided into two stages according to the leaching rate. The first 21 h of leaching can be considered as the first stage, in which copper extraction increased rapidly as a straight line. The stage after 21 h of leaching can be regarded as the second stage, in which copper extraction increased much slower than the first stage. It was reported that the first stage was controlled by the diffusion of oxidant and the activation energy was 4–25 KJ/mol, whilst the activation energy of the second stage was 55–105 KJ/mol [22,30], which was considered as the main reason of the difference in copper extraction.

The variation of iron ion concentration in the first 15 h of chalcocite leaching is shown in Figure 2b. It indicated that the concentration of iron ions had a sudden decrease at the first 1 h of leaching, and then it increased slowly until leaching for 10 h, and thereafter remained stable. It has been reported that ferric ions have a stronger oxidizing ability than dissolved oxygen [46], hence the direct oxidant in chalcocite acidic ferric sulfate leaching was ferric ions. Although iron ions may hydrolyze to form a precipitate due to pH changes during leaching, the amount was small near the pH value of 2.0. Accordingly, it can be speculated that ferric ions in solution may have directly reacted with chalcocite and generated some iron-containing compounds in the first 1 h of leaching, and after 10 h of leaching, the generated iron-containing compounds were dissolved again.

Figure 2c,d shows the variations of pH value and redox potential, respectively. It revealed that pH value had a significant increase, whilst redox potential had a sharp decrease at the beginning of the leaching. This can be attribute to the rapid consumption of sulfuric acid shown by Equation (3), and the rapid consumption of ferric ions as follows in Equations (1) and (2).

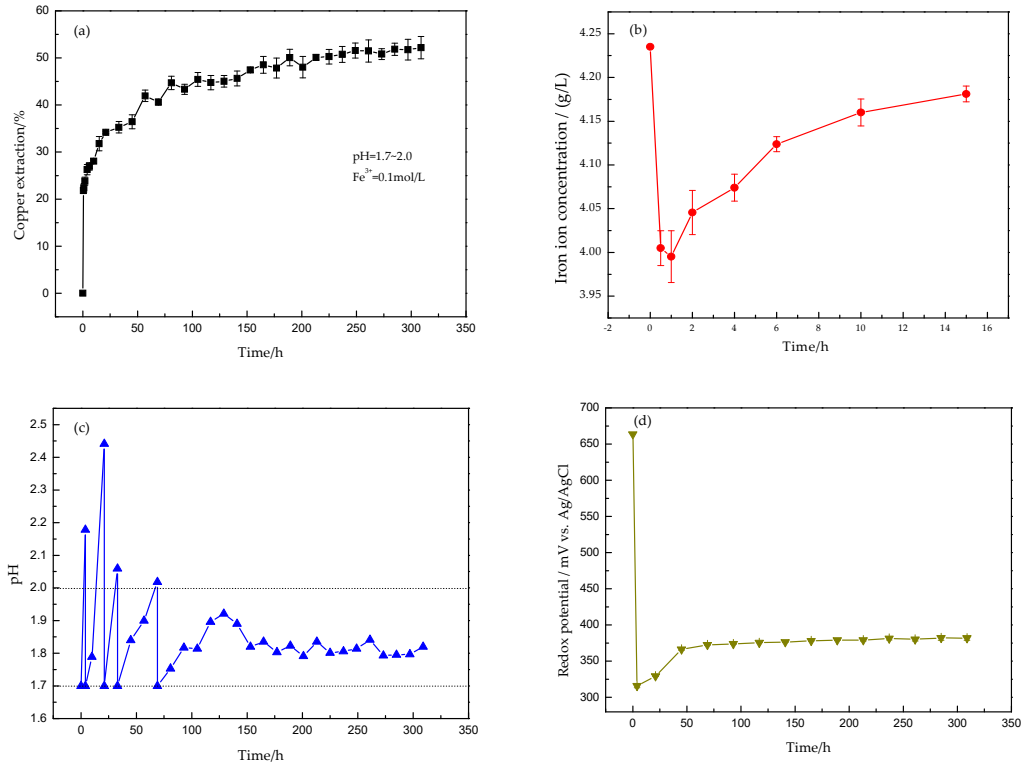

Figure 2. Results of chalcocite acidic ferric sulfate leaching (pH = 1.7~2.0, C(Fe^{3+}) = 0.1 mol/L): (**a**) Copper extraction at different leaching times; (**b**) Iron ion concentration in the first 15 h; (**c**) Variation of pH value; (**d**) Variations of redox potential.

3.2. Synchrotron Radiation X-ray Diffraction Tests

3.2.1. SRXRD Results of the First Stage of Leaching

To further investigate the phase transformation process of the first stage of chalcocite leaching, SRXRD was used to analyze the intermediate species during chalcocite leaching. Figure 3 and Table 2 show that chalcocite disappeared just after half an hour of leaching, while $Cu_{7.2}S_4$, $Cu_{1.8}S$, Cu_8S_5, and Cu_5FeS_4 were detected by SRXRD. It indicated that chalcocite was quickly oxidized in the initial stage of ferric leaching and some intermediates were generated. Afterwards, no new phase appeared and the peak intensity of $Cu_{7.2}S_4$ decreased when leached for 1 h, which indicated part dissolution of $Cu_{7.2}S_4$.

However, CuS appeared as an intermediate when chalcocite was leached for 2 h, whilst the peak intensity of $Cu_{7.2}S_4$ and Cu_5FeS_4 experienced a decrease. Then, the peak intensity of $Cu_{7.2}S_4$ disappeared when leached for 4 h, and the peak intensity of Cu_8S_5 was when leached for 6 h. Moreover, the peak intensity of Cu_5FeS_4 was increasingly weaker, whilst the peak intensity of CuS became increasingly stronger as chalcocite was leached for 2 h to 6 h.

After leaching for 10 and 15 h, Cu_5FeS_4 disappeared and elemental sulfur was generated, which indicated that the generated intermediate Cu_5FeS_4 had dissolved after 10 h of leaching, and that part of CuS had oxidized to elemental sulfur.

According to Figure 3, it can be concluded that the first stage of chalcocite leaching was not a simple process where Cu^{2+} dissolved into solution and chalcocite directly transformed to CuS. Instead, it was a complex and fast process in which several chemical reactions occurred simultaneously. The products of these reactions were several similar minerals containing Cu, S, or Fe elements, which are close to each other in diffraction peak. In particular, Cu_5FeS_4 was detected for the first time by SRXRD, which was in accordance with the results of Figure 2b. It will be helpful for explaining the phase transformation mechanism in chalcocite leaching.

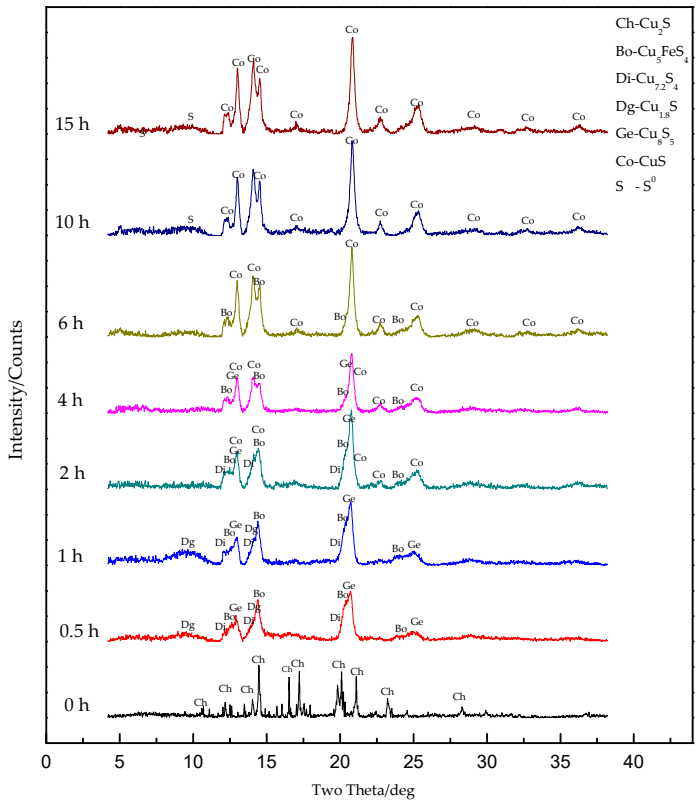

Figure 3. SRXRD results of the phase transformation process in the first stage of chalcocite acidic ferric sulfate leaching (Shanghai Synchrotron Radiation Facility (SSRF)).

Table 2. The minerals detected in different leaching time.

Time/h	Cu_2S	Cu_5FeS_4	$Cu_{1.8}S$	$Cu_{7.2}S_4$	Cu_8S_5	CuS	S
0	√						
0.5		√	√	√	√		
1		√	√	√	√		
2		√		√	√	√	
4		√			√	√	
6		√				√	
10						√	√
15						√	√

3.2.2. SRXRD Results of the Second Stage of Chalcocite Leaching

The results shown in Figure 4 suggest that no new phase appeared in the second stage of chalcocite leaching, where the peak intensity of CuS was increasingly weaker, whilst the peak intensity of elemental sulfur was increasingly stronger as the leaching continued. After leaching for 933 h, the main phase was elemental sulfur and only a few CuS existed.

Equation (2) shows that the second stage of chalcocite leaching was the redox reaction between covellite and ferric ions. In this process, ferric ions acted as an oxidant reduced to ferrous ions, whilst CuS was oxidized to elemental sulfur. Meanwhile, it should be noted that only a small amount of elemental sulfur would be continuously oxidized to sulfate under low redox potential, as shown in Figure 2d [30].

Hence, it can be concluded that in the second stage of chalcocite acidic ferric sulfate leaching, CuS was transformed to elemental sulfur and no new intermediate was generated. However, it should be noted that the kinetics of the second stage of chalcocite leaching were much lower than the first stage. The reason may be that the generated elemental sulfur formed a passivation layer and inhibited the dissolution of chalcocite.

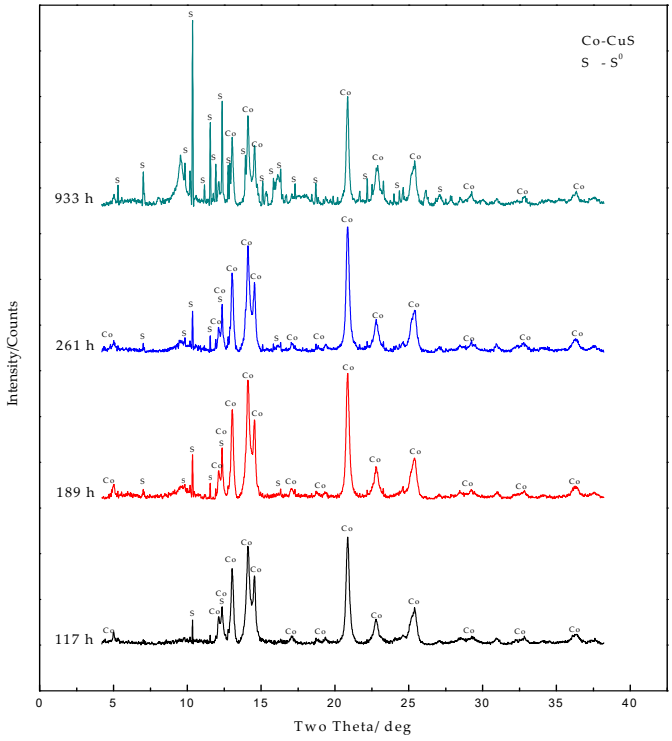

Figure 4. SRXRD results of the phase transformation process in the second stage of chalcocite acidic ferric sulfate leaching (SSRF).

3.3. Thermodynamic Calculation of the Generation and Dissolution of Cu_5FeS_4 in Chalcocite Leaching Process

Whether a reaction can start spontaneously depends on the variation of Gibbs free energy of the reaction. If the variation of Gibbs free energy of the reaction was negative, the reaction can be spontaneously started. On the contrary, the reaction cannot be carried out spontaneously.

According to the redox properties of various chemical components in the leaching process, it can be inferred that Cu_5FeS_4 detected by SRXRD might be generated and dissolved, as shown in Equations (4) and (5).

$$4Cu_2S + 4Fe^{3+} \rightarrow Cu_5FeS_4 + 3Cu^{2+} + 3Fe^{2+} \quad (4)$$

$$Cu_5FeS_4 + 4Fe^{3+} \rightarrow 4CuS + Cu^{2+} + 5Fe^{2+} \quad (5)$$

Some thermodynamic data are listed in Table 3. The variations of Gibbs free energy can be calculated from Equation (6):

$$\Delta_r G_m = \Delta_r G_m^{\Theta} + RTlnK \quad (6)$$

where K was the chemical reaction equilibrium constant.

According to the thermodynamic data in Table 3, it can be calculated that the variations of Gibbs free energy of Equations (4) and (5) were −69.62 KJ/mol and −113.63 KJ/mol under standard state, respectively. It indicated that Equations (4) and (5) can be carried out spontaneously on thermodynamics by Gibbs free energy criterion.

Table 3. Some standard thermodynamic data (298.15 K) [47,48].

Components	Enthalpy (KJ/mol)	Entropy (J/mol/K)	Gibbs Free Energy (KJ/mol) (298.15 K)
Cu_2S	−79.496	120.918	−115.548
Cu_5FeS_4	−380.326	362.334	−488.356
CuS	−48.530	66.530	−68.366
Cu^{2+} (aq)	64.768	−99.579	94.458
Fe^{3+} (aq)	−48.534	−315.892	45.649
Fe^{2+} (aq)	−89.119	−137.654	−48.078

3.4. Disscussion of the Fine Phase Transformation of Chalcocite Acidic Ferric Sulfate Leaching

In the leaching process in acidic ferric sulfate solution, chalcocite was firstly reacted with ferric ions and some intermediates $Cu_{1.8}S$, $Cu_{7.2}S_4$, Cu_8S_5, and Cu_5FeS_4 were generated according to Equations (7) and (4). Then, $Cu_{1.8}S$, $Cu_{7.2}S_4$, and Cu_8S_5 were oxidized to CuS in that order, according to Equation (8). Afterwards, Cu_5FeS_4 was also oxidized to CuS, following Equation (5). Finally, CuS was oxidized to elemental sulfur, following Equation (2). Meanwhile, ferric ions played the role of oxidants during the entire leaching process and were regenerated in accordance with Equation (3).

$$Cu_2S + 2xFe^{3+} \rightarrow Cu_{2-x}S + xCu^{2+} + 2xFe^{2+}, (0 < x < 1) \quad (7)$$

$$Cu_{2-x}S + 2(1-x)Fe^{3+} \rightarrow CuS + (1-x)Cu^{2+} + 2(1-x)Fe^{2+}, (0 < x < 1) \quad (8)$$

It should be noting that the disappearance of those intermediates was in the order of $Cu_{1.8}S \rightarrow Cu_{7.2}S_4 \rightarrow Cu_8S_5 \rightarrow Cu_5FeS_4 \rightarrow CuS$, according to Figures 3 and 4. In addition, it has been reported by many researchers that there exists a galvanic effect between different semiconductor minerals when they are leached [49–51]. In the first stage of chalcocite leaching, several copper sulfide minerals appeared; the other potentials of these minerals were different and there existed a galvanic effect between them. The other potentials of these minerals were in the following order: $Cu_2S < Cu_{1.8}S < Cu_{1.6}S < Cu_5FeS_4 < CuS$. Hence, it can be speculated that the galvanic effect between Cu_5FeS_4 and $Cu_{2-x}S$ accelerated the dissolution of Cu_2S and $Cu_{2-x}S$, and when $Cu_{2-x}S$ was completely transformed to CuS, a galvanic effect between Cu_5FeS_4 and CuS accelerated the dissolution of Cu_5FeS_4, then all the intermediates were transformed to CuS.

Therefore, it can be concluded that the probable phase transformation mechanism of chalcocite leaching in acidic ferric solution is as shown in Figure 5.

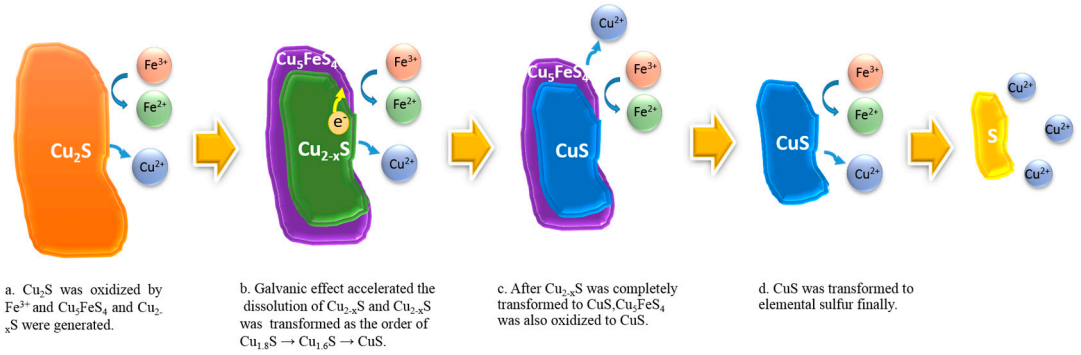

Figure 5. Probable fine phase transformation during chalcocite acidic ferric sulfate leaching.

4. Conclusions

In summary, the acidic ferric sulfate leaching of synthetic chalcocite was divided into two stages. Chalcocite was transformed to covellite in the first stage, then covellite was transformed to elemental sulfur in the second stage. Meanwhile, the kinetic of the second stage was much lower than the first stage.

However, the fine phase transformation process of synthetic chalcocite acidic ferric sulfate leaching was a complicated process involving Cu, Fe, and S elements:

(1) Firstly, chalcocite reacted with Fe^{3+} and was quickly transformed to $Cu_{7.2}S_4$, $Cu_{1.8}S$, Cu_8S_5, and Cu_5FeS_4.

(2) Then, the galvanic effect between Cu_5FeS_4 and $Cu_{2-x}S$ accelerated the dissolution of $Cu_{2-x}S$, and the phase transformation order of $Cu_{2-x}S$ was $Cu_{1.8}S \rightarrow Cu_{1.6}S \rightarrow CuS$.

(3) When $Cu_{2-x}S$ was completely transformed to CuS, Cu_5FeS_4 was transformed to CuS thereafter.

(4) In the second stage, the generated CuS was oxidized to elemental sulfur, which should be the passivation layer inhibiting the efficient leaching of chalcocite.

Author Contributions: Conceptualization, W.Q., G.Q. and J.W.; Data curation, C.F., S.Y. and X.W.; Formal analysis, C.F., H.Z. and J.W.; Funding acquisition, C.F., H.Z. and J.W.; Investigation, C.F., S.Y. and X.W.; Methodology, C.F.; Project administration, J.W.; Resources, J.W.; Software, C.F., S.Y. and X.W.; Writing—original draft, C.F.; Writing—review & editing, H.Z., W.Q. and J.W.

Funding: This research was funded by Natural Science Foundation of Hunan Province (No. 2018JJ1041), the National Natural Science Foundation of China (No. 51774332, 51320105006, 51704331 and 51374248), Hunan Provincial Innovation Foundation for Postgraduate (CX2018B067), CSU Special Scholarship for Study Abroad (2018154), Innovation-Driven Project of Central South University (2018CX019) and National Undergraduate Innovation and Entrepreneurship Training Program (201810533348).

Acknowledgments: Authors acknowledge the staff and other professors at beamline 4B9A of the Beijing Synchrotron Radiation Facility (BSRF) and beamline BL14B1 at the Shanghai Synchrotron Radiation Facility (SSRF) for their help in beamline operation, data collection, and direction.

Conflicts of Interest: The authors declare no conflict of interest.

References

1. Chen, X.M.; Peng, Y.J.; Bradshaw, D. The separation of chalcopyrite and chalcocite from pyrite in cleaner flotation after regrinding. *Miner. Eng.* **2014**, *58*, 64–72. [CrossRef]
2. Qin, W.Q.; Wu, J.J.; Jiao, F.; Zeng, J.M. Mechanism study on flotation separation of molybdenite from chalcocite using thioglycollic acid as depressant. *Int. J. Min. Sci. Technol.* **2017**, *27*, 1043–1049. [CrossRef]
3. Gao, Y.S.; Gao, Z.Y.; Sun, W.; Yin, Z.G.; Wang, J.J.; Hu, Y.Y. Adsorption of a novel reagent scheme on scheelite and calcite causing an effective flotation separation. *J. Colloid Interface Sci.* **2018**, *512*, 39–46. [CrossRef] [PubMed]

4. Li, C.W.; Gao, Z.Y. Effect of grinding media on the surface property and flotation behavior of scheelite particles. *Powder Technol.* **2017**, *322*, 386–392. [CrossRef]
5. Brierley, J.A.; Brierley, C.L. Present and future commercial applications in biohydrometallurgy. *Hydrometallurgy* **2001**, *59*, 233–240. [CrossRef]
6. Zhao, H.B.; Wang, J.; Hu, M.H.; Qin, W.Q.; Zhang, Y.S.; Qiu, G.Z. Synergistic bioleaching of chalcopyrite and bornite in the presence of *Acidithiobacillus ferrooxidans*. *Bioresour. Technol.* **2013**, *149*, 71–76. [CrossRef] [PubMed]
7. Zhao, H.B.; Wang, J.; Gan, X.W.; Zheng, X.H.; Tao, L.; Hu, M.H.; Li, Y.N.; Qin, W.Q.; Zhang, Y.S.; Qiu, G.Z. Effects of pyrite and bornite on bioleaching of two different types of chalcopyrite in the presence of *Leptospirillum ferriphilum*. *Bioresour. Technol.* **2015**, *194*, 28–35. [CrossRef] [PubMed]
8. Lan, Z.Y.; Hu, Y.H.; Liu, J.S.; Wang, J. Solvent extraction of copper and zinc from bioleaching solutions with LIX984 and D2EHPA. *J. Cent. South Univ. Technol.* **2005**, *12*, 45–49. [CrossRef]
9. Wang, J.; Zhao, H.B.; Zhuang, T.; Qin, W.Q.; Zhu, S.; Qiu, G.Z. Bioleaching of Pb–Zn–Sn chalcopyrite concentrate in tank bioreactor and microbial community succession analysis. *Trans. Nonferrous Met. Soc. China* **2013**, *23*, 3758–3762. [CrossRef]
10. Wang, J.; Zhu, S.; Zhang, Y.S.; Zhao, H.B.; Hu, M.H.; Yang, C.R.; Qin, W.Q.; Qiu, G.Z. Bioleaching of low-grade copper sulfide ore by *Acidithiobacillus ferrooxidans* and *Acidithiobacillus thiooxidans*. *J. Cent. South Univ.* **2014**, *21*, 728–734. [CrossRef]
11. Zhao, H.B.; Huang, X.T.; Hu, M.H.; Zhang, C.Y.; Zhang, Y.S.; Wang, J.; Qin, W.Q.; Qiu, G.Z. Insights into the surface transformation and electrochemical dissolution process of bornite in bioleaching. *Minerals* **2018**, *8*, 173. [CrossRef]
12. Michael, N.; Petrus, B. The anodic behavior of covellite in chloride solutions. *Hydrometallurgy* **2017**, *172*, 60–68.
13. Bolorunduro, S.A. Kinetics of Leaching of Chalcocite in Acid Ferric Sulfate Media: Chemical and Bacterial Leaching. Master's Thesis, University of Brithsh Columbia, Vancouver, BC, Canada, 1999.
14. Brierley, C.L. A perspective on developments in biohydrometallurgy. *Hydrometallurgy* **2008**, *94*, 2–7. [CrossRef]
15. Brierley, C.L. Biohydrometallurgical prospects. *Hydrometallurgy* **2010**, *104*, 324–328. [CrossRef]
16. Buerger, M.J.; Wuensch, B.J. Distribution of atoms in high chalcocite, Cu_2S. *Science* **1963**, *141*, 276–277. [CrossRef] [PubMed]
17. Howard, T.; Evans, J. The crystal structure of low chalcocite and djurleite. *Z. Krist.* **1979**, *150*, 299–320.
18. Evans, J.; Howard, T. Djurleite ($Cu_{1.94}S$) and Low Chalcocite (Cu_2S): New Crystal Structure Studies. *Science* **1979**, *203*, 356–358. [CrossRef] [PubMed]
19. Howard, T.; Evans, J. Copper coordination in low chalcocite and djurleite and other copper-rich sulfides. *Am. Miner.* **1981**, *66*, 807–818.
20. Sullivan, J.D. *Chemistry of Leaching Chalcocite*; US Bureau of Mines: Washington, DC, USA, 1930; p. TP 473.
21. Fisher, W.W.; Flores, F.A.; Henderson, J.A. Comparison of chalcocite dissolution in the oxygenated, aqueous sulfate and chloride systems. *Miner. Eng.* **1992**, *7*, 817–834. [CrossRef]
22. Peterson, J.; Dixon, D.G. The dynamics of chalcocite heap bioleaching. In *Hydrometallurgy 2003: Fifth International Conference in Honor of Professor Lan M. Ritchie*; TMS: Pittsburgh, PA, USA, 2003; pp. 351–364.
23. Ruiz, M.C.; Abarzua, E.; Padilla, R. Oxygen pressure leaching of white metal. *Hydrometallurgy* **2007**, *86*, 131–139. [CrossRef]
24. Miki, H.; Nicol, M.; Velásquez-Yévenes, L. The kinetics of dissolution of synthetic covellite, chalcocite and digenite in dilute chloride solutions at ambient temperatures. *Hydrometallurgy* **2011**, *105*, 321–327. [CrossRef]
25. Ruan, R.M.; Zou, G.; Zhong, S.P.; Wu, Z.L.; Chan, B.; Wang, D.Z. Why Zijinshan copper bioheapleaching plant works efficiently at low microbial activity—Study on leaching kinetics of copper sulfides and its implications. *Miner. Eng.* **2013**, *48*, 36–43. [CrossRef]
26. Niu, X.P.; Ruan, R.M.; Tan, Q.Y.; Jia, Y.; Sun, H.Y. Study on the second stage of chalcocite leaching in column with redox potential control and its implications. *Hydrometallurgy* **2015**, *155*, 141–152. [CrossRef]
27. Cavallotti, P.; Salvago, G. Electronic Behavior of Copper Sulfides in Aqueous Solutions. *Electrochim. Metallorum* **1969**, *4*, 181–210.
28. Moh, G.H. Blue remaining covellite and its relations to phases in the sulfur rich portion of the copper-sulfur System at low temperatures. *Miner. Soc. Jpn.* **1971**, *1*, 180–188.

29. Whiteside, L.S.; Goble, R.J. Structural and compositional changes in copper sulfides during leaching and dissolution. *Can. Mineral.* **1986**, *24*, 247–258.
30. Cheng, C.Y.; Lawson, F. The kinetics of leaching chalcocite in acidic oxygenated sulphat-chloride solutions. *Hydrometallurgy* **1991**, *27*, 249–268. [CrossRef]
31. Zhao, H.B.; Wang, J.; Yang, C.R.; Hu, M.H.; Gan, X.W.; Tao, L.; Qin, W.Q.; Qiu, G.Z. Effect of redox potential on bioleaching of chalcopyrite by moderately thermophilic bacteria: An emphasis on solution compositions. *Hydrometallurgy* **2015**, *151*, 141–150. [CrossRef]
32. Dutrizac, J. Elemental sulphur formation during the ferric sulphate leaching of chalcopyrite. *Can. Metall. Q.* **1989**, *28*, 337–344. [CrossRef]
33. Dutrizac, J. Elemental sulphur formation during the ferric chloride leaching of chalcopyrite. *Hydrometallurgy* **1990**, *23*, 153–176. [CrossRef]
34. Klauber, C. A critical review of the surface chemistry of acidic ferric sulphate dissolution of chalcopyrite with regards to hindered dissolution. *Int. J. Miner. Process.* **2008**, *86*, 1–17. [CrossRef]
35. Zhao, H.B.; Hu, M.H.; Li, Y.N.; Zhu, S.; Qin, W.Q.; Qiu, G.Z.; Wang, J. Comparison of electrochemical dissolution of chalcopyrite and bornite in acid culture medium. *Trans. Nonferrous Met. Soc. China* **2015**, *25*, 303–313. [CrossRef]
36. Zhao, H.B.; Wang, J.; Gan, X.W.; Hu, M.H.; Tao, L.; Qin, W.Q.; Qiu, G.Z. Role of pyrite in sulfuric acid leaching of chalcopyrite: An elimination of polysulfide by controlling redox potential. *Hydrometallurgy* **2016**, *164*, 159–165. [CrossRef]
37. Zhao, H.B.; Wang, J.; Qin, W.Q.; Hu, M.H.; Zhu, S.; Qiu, G.Z. Electrochemical dissolution process of chalcopyrite in the presence of mesophilic microorganisms. *Miner. Eng.* **2015**, *71*, 159–169. [CrossRef]
38. Qin, W.Q.; Wang, J.; Zhang, Y.S.; Zhen, S.J.; Shang, H.; Liu, Q.; Qiu, G.Z. Electrochemical behavior of massive bornite bioleached electrodes in the presence of Acidithiobacillus ferrooxidans and *Acidithiobacillus caldus*. *Adv. Mater. Res.* **2009**, *71*, 417–420. [CrossRef]
39. Liu, H.C.; Xia, J.L.; Nie, Z.Y. Comparative study of S, Fe and Cu speciation transformation during chalcopyrite bioleaching by mixed mesophiles and mixed thermophiles. *Miner. Eng.* **2017**, *106*, 22–32. [CrossRef]
40. Yang, Y.; Harmer, S.; Chen, M. Synchrotron X-ray photoelectron spectroscopic study of the chalcopyrite leached by moderate thermophiles and mesophiles. *Miner. Eng.* **2014**, *69*, 185–195. [CrossRef]
41. Acres, R.G.; Harmer, S.L.; Beattie, D.A. Synchrotron XPS studies of solution exposed chalcopyrite, bornite, and heterogeneous chalcopyrite with bornite. *Int. J. Miner. Process.* **2010**, *94*, 43–51. [CrossRef]
42. Majuste, D.; Ciminelliv, S.T.; Eng, P.J. Applications of in situ synchrotron XRD in hydrometallurgy: Literature review and investigation of chalcopyrite dissolution. *Hydrometallurgy* **2013**, *131*, 54–66. [CrossRef]
43. Fang, J.H.; Liu, Y.; He, W.L.; Qin, W.Q.; Qiu, G.Z.; Wang, J. Transformation of iron in pure culture process of extremely acidophilic microorganisms. *Trans. Nonferrous Met. Soc. China* **2017**, *27*, 1150–1155. [CrossRef]
44. Wang, X.X.; Liao, R.; Zhao, H.B.; Hong, M.X.; Wang, J. Synergetic effect of pyrite on strengthening bornite bioleaching by *Leptospirillum ferriphilum*. *Hydrometallurgy* **2017**, *176*, 9–16. [CrossRef]
45. Fang, C.J.; Chang, Z.Y.; Feng, Q.M.; Xiao, W.; Yu, S.C.; Qiu, G.Z.; Wang, J. The influence of backwater Al^{3+} on diaspore bauxite flotation. *Minerals* **2017**, *7*, 195. [CrossRef]
46. Zhao, H.B.; Wang, J.; Tao, L.; Cao, P.; Yang, C.R.; Qin, W.Q.; Qiu, G.Z. Roles of oxidants and reductants in bioleaching system of chalcopyrite at normal atmospheric pressure and 45 °C. *Int. J. Miner. Process.* **2017**, *162*, 81–91. [CrossRef]
47. Liang, Y.; Che, Y. *Inorganic Thermodynamic Data Manual*, 1st ed.; Northeastern University Press: Shenyang, China, 1993; pp. 39–441.
48. Dean, J.A. *Lange's Handbook of Chemistry*, 12th ed.; MvGrew-Hill: New York, NY, USA, 1979; pp. 9–94.
49. Wu, B.; Yang, X.L.; Cai, L.L.; Yao, G.C.; Wen, J.K.; Wang, D.Z. The influence of pyrite on galvanic assisted leaching of chalcocite concentrates. *Adv. Mater. Res.* **2013**, *825*, 459–463. [CrossRef]
50. Javad Koleini, S.M.; Jafarian, M.; Abdollahy, M.; Aghazadeh, V. Galvanic leaching of chalcopyrite in atmospheric pressure and sulfate media: Kinetic and surface studies. *Ind. Eng. Chem. Res.* **2010**, *49*, 5997–6002. [CrossRef]
51. Huai, Y.Y.; Plackowski, C.; Peng, Y.J. The galvanic interaction between gold and pyrite in the presence of ferric ions. *Miner. Eng.* **2018**, *119*, 236–243. [CrossRef]